THREE-DIMENSIONAL NUMERICAL MODELING FOR THE MOTION OF STONES WITH DIFFERENT SIZES AND SHAPES IN STREAMS

Tomoo Fukuda [1], Shoji Fukuoka [2] and Tatsuhiko Uchida[3]

ABSTRACT

The moving mechanism of stones with different sizes and shapes in streams is required to evaluate the sediment transport rate and bed variation in gravel bed rivers. One of the authors made a real scale experiment of stones moving in streams and measured moving trajectories of stones. In this paper, a three-dimensional numerical model is presented which simulates the motions of a cloud of stones with different sizes and shapes in streams. The validation of the model is checked by the real scale experiment. And the mechanism of stones moving in streams is discussed by using the results of the real scale experiment and the simulation. It is demonstrated that shapes of stones are important for estimating their motion in streams, and the motions of stones containing just a few percent of volume density in streams have significant effects on momentum transport of the flow in the vertical direction.

1. INTRODUCTION

The moving mechanism of stones in streams is required to estimate the sediment transport rate and bed variation in gravel bed rivers. Generally, bed materials in gravel bed rivers are widely distributed in size and in shape. Therefore, regarding the mechanism of stones moving in streams, it is important to elucidate effects of size and shape of stones on collisions between stones and interaction between stones and water. Fukuoka et al. (2005) made a real scale experiment of a cloud of stones moving in streams with a 45m long concrete channel and measured moving trajectories of colored stones by using image analyses (hereinafter referred to as the real scale experiment). It has been indicated that stones shapes have significant effects on their irregular saltations and migration. In order to elucidate the dynamic mechanism of stones moving in streams, the authors develop a three-dimensional numerical model, in which the motion of each shaped stone is simulated with the Lagrangian method and fluid motion around stones are simulated directly with the Eulerian method.

[1] Graduate student, Department of Science and Engineering, Chuo University 1-13-27 Kasuga, Bunkyo-ku, Tokyo, 112-8551, Japan (t-fukuda66@civil.chuo-u.ac.jp)
[2] Professor, Research and Development Initiative, Chuo University, 1-13-27 Kasuga, Bunkyo-ku, Tokyo, 112-8551, Japan (sfuku@tamacc.chuo-u.ac.jp)
[3] Associate Professor, Research and Development Initiative, Chuo University, 1-13-27 Kasuga, Bunkyo-ku, Tokyo, 112-8551, Japan (utida@tamacc.chuo-u.ac.jp)

Figure 1 Combined stone model

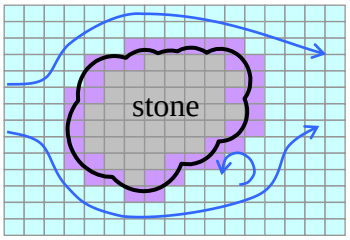

Figure 2 Concept of the fluid analysis

Many previous studies on a numerical computation of stones moving in streams had attempted to evaluate hydrodynamic forces based on empirical coefficients (e.g. Gotoh et al., 2000). However, drag coefficients of various shaped stones moving in the cloud has remained unknown. On the other hand, numerical methods have been proposed to evaluate the interaction between fluid flow and arbitrary shaped solid objects in which fluid motions around stones and hydrodynamic forces are calculated directly by using small computational cells (e.g. Ushijima et al., 2008).

A rigid body composed of tetrahedron elements has been used as an arbitrary shaped object (Suzuki et al., 2003). Although the combined tetrahedron elements model is suitable to evaluate rigid body properties such as mass, gravity center and moment of inertia, proper numerical procedures are required to detect positions of contacts and collisions between objects. Matsushima et al. (2004) proposed the stone model of combined spheres to evaluate contact forces easily by radii and the distance between two spheres. However combined sphere model has difficulties in calculation of rigid body properties due to overlapped spheres.

The authors developed the three-dimensional numerical model for multiphase flow with stones of different sizes and shapes moving in streams in which the combined spheres are used as stones model (Figure 1) and hydrodynamic forces of stones are calculated directly. In the model, stones motions are simulated as rigid body. We evaluated rigid body properties of stones consist of combined spheres by numerical integrations with sufficiently small cells around and in a stone. The most distinctive features of the present numerical model are in the ability to investigate dynamic interaction between a cloud of irregular shaped stones and water in detail which is impossible to measure in experimental channels and fields.

2. NUMERICAL MODEL

In the present numerical model, fluid motions are simulated with the Eaulerian method and stones motions are simulated with the Lagrangian method. To take into account the effect of solid phase on liquid phase, fluid motions are simulated by governing equations of multiphase flow (Figure 2). Fluid forces acting on stones are evaluated directly by integrating the equations for multiphase flow motion. The Discrete Elements Method (Cundall and Strack, 1979) is applied to simulate motions of arbitrary shaped stones. Arbitrary shapes of stones are made by combinations of several small spheres (Figure 1). The motions of the stones are simulated by momentum and angular momentum equations for a rigid body.

2.1 Governing Equation of Fluid Motion

Fluid motion is simulated by one-fluid model for multiphase flow using Smagorinsky model as the subgrid turbulence model:

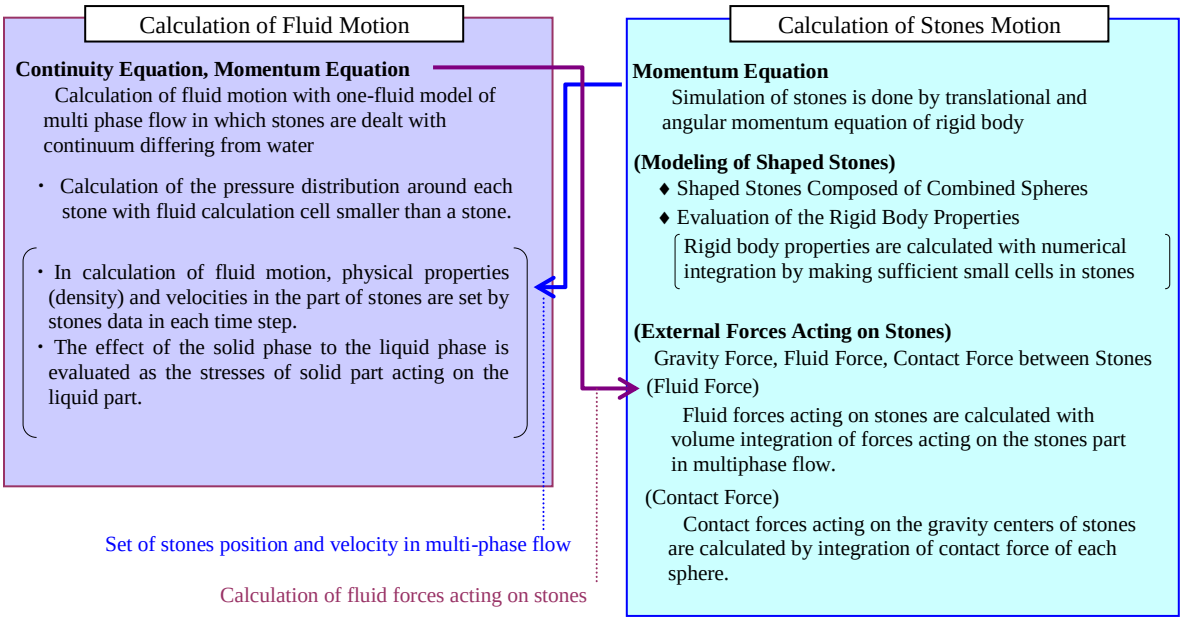

Figure 3 Concept of simulation model for stones moving in streams

$$\frac{\partial u_i}{\partial x_i} = 0 \tag{1}$$

$$\frac{\partial u_i}{\partial t} + u_j \frac{\partial u_i}{\partial x_j} = F_i - \frac{1}{\rho}\frac{\partial P}{\partial x_i} + (\nu + \nu_t)\left(\frac{\partial^2 u_i}{\partial x_j \partial x_j}\right) \tag{2}$$

$$\nu = \mu/\rho\,, \qquad \nu_t = (C_S\Delta)^2\sqrt{2S_{ij}S_{ij}}\,, \qquad S_{ij} = \frac{1}{2}\left(\frac{\partial u_i}{\partial x_j} + \frac{\partial u_j}{\partial x_i}\right) \tag{3}$$

$$\phi = \alpha\phi_s + (1-\alpha)\phi_f\,, \quad \phi_f = f\phi_l + (1-f)\phi_g \tag{4}$$

$$u_i = \{\alpha\rho_s u_{si} + (1-\alpha)\rho_l u_{li}\}/\rho \tag{5}$$

where u_i :density-weighted average in fluid velocity , P : normal stress, Δ : calculation grid size, f :fluid and solid volume fraction in fluid calculation cell, α :solid volume fraction in fluid calculation cell except gas part, ϕ :physical property (density ρ , coefficient of dynamic viscosity μ), suffix l , s and g denote liquid phase, solid phase and gas phase, respectively. Continuity equation and momentum equations are solved by the SMAC scheme with staggered grid.

Water surface is evaluated with volume fraction of fluid f in fluid calculation cell based on the VOF method (Hirt and Nichols, 1981).

$$\frac{\partial f}{\partial t} + \frac{\partial f u_i}{\partial x_i} = 0 \tag{6}$$

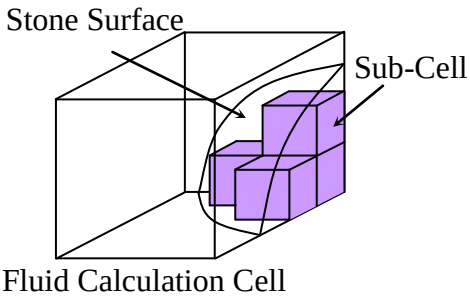

Figure 4 Evaluation of stones volume with sub-cell

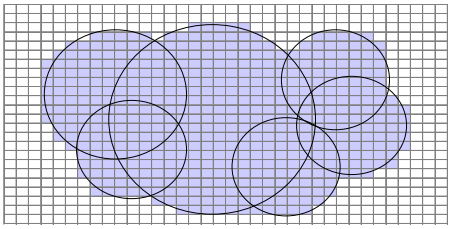

Figure 5 Cells image for calculation of rigid body properties

Solid motion in fluid flow is recognized and calculated by u_i and physical property ϕ which are set in considering solid volume fraction in fluid calculation cell by eq. (4) and eq. (5). Solid velocity u_s in eq. (5) is calculated equation below:

$$\boldsymbol{u}_s = \dot{\boldsymbol{r}}_G + \boldsymbol{\omega} \times \boldsymbol{r}_f \tag{7}$$

where $\dot{\boldsymbol{r}}_G$:translational velocity vector of stones (velocity at the gravity center), $\boldsymbol{\omega}$:rotational velocity vector of stones, $\boldsymbol{r}_f$:position vector from gravity center to the evaluation point of $\boldsymbol{u}_s$.

The solid volume fraction in fluid calculation cell α in eq. (4) and eq. (5) is calculated with using sub-cells splitting a fluid calculation cell (shown in Figure 4).

2.2 Modeling of Arbitrary Shaped Stones

Arbitrary shapes of stones are made by the combination of several small spheres to detect contact and collision points between stones as seen in Figure 1. On the other hand, it is difficult to evaluate geometries of lapped part of spheres. We propose the numerical integration for calculating rigid body properties of stones by using small cells in stones (shown in Figure 5). The rigid body properties of stones in motion are not changed, therefore the calculation of rigid body properties needs to be done just once at the beginning of the simulation.

2.3 Governing Equation of Stone Motion in Streams

Irregular shaped stones motions are simulated by translational and rotational equations of motion for the rigid body:

$$M\ddot{\boldsymbol{r}}_G = M\boldsymbol{g} + \boldsymbol{F}_f + \boldsymbol{F}_c \tag{8}$$

$$\dot{\boldsymbol{\omega}}_r = \boldsymbol{I}_r{}^{-1}\left(\boldsymbol{R}^{-1}\boldsymbol{N} - \boldsymbol{\omega}_r \times \boldsymbol{I}_r\boldsymbol{\omega}_r\right), \qquad \boldsymbol{N} = \boldsymbol{N}_f + \boldsymbol{N}_c \tag{9}$$

where $\ddot{\boldsymbol{r}}_G$:translational acceleration vector of stones, suffix f , c : fluid force, contact force between stones, respectively, suffix r :components in local coordinate systems of each stone, $\boldsymbol{R}$:translational tensor from the global coordinate system to the local coordinate system and $\boldsymbol{I}$:tensor of momentum inertia. After the calculation of rotational velocity in local coordinate system $\boldsymbol{\omega}_r$ in eq. (9), rotational velocity $\boldsymbol{\omega}$ in global coordinate system is solved by coordinate transformation. In calculation of

coordinate transformation from the local coordinate system of the stone to the global coordinate system, the quaternion is used in stead of translational tensor $\boldsymbol{R}$ (Ushijima et al., 2008).

2.4 Evaluation of Fluid Force

Fluid forces acting on the stones are evaluated with integrating pressure and shear stress terms of eq. (2) in the stones volume (Ushijima et al., 2008):

$$F_{f,i} = \int_{\Omega_s} \left\{ -\frac{\partial P}{\partial x_i} + \rho(\nu + \nu_t) \left(\frac{\partial^2 u_i}{\partial x_j \partial x_j} \right) \right\} d\Omega \tag{10}$$

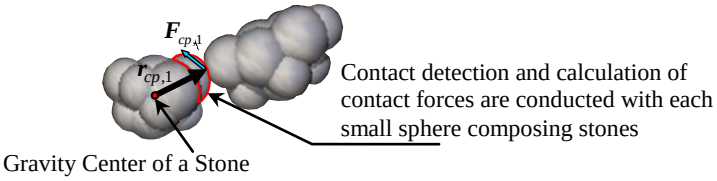

Figure 6 Evaluation of contact forces

$$N_{f,i} = \int_{\Omega_s} \varepsilon_{ijk} r_{f,j} \left\{ -\frac{\partial P}{\partial x_k} + \rho(\nu + \nu_t) \left(\frac{\partial^2 u_k}{\partial x_l \partial x_l} \right) \right\} d\Omega \tag{11}$$

where $F_{f,i}$: i component of fluid force, $N_{f,i}$: i component of torque caused by fluid force, $r_{f,i}$: position vector from the gravity center of stone to the fluid calculation cells, Ω_s : an area occupied by a stone and ε_{ijk} Levi-Civita symbol.

2.5 Evaluation of Contact Force

Contact forces acting between stones are calculated by small spheres forming a shaped stone(shown in Figure 6). The forces and torques acting on stones are calculated by the summation of the contact forces:

$$\boldsymbol{F}_c = \Sigma \boldsymbol{F}_{cp,n}, \quad \boldsymbol{N}_c = \Sigma \boldsymbol{r}_{cp,n} \times \boldsymbol{F}_{cp,n} \tag{12}$$

where $\boldsymbol{F}_c$, $\boldsymbol{N}_c$: contact force and torque, $\boldsymbol{F}_{cp,n}$:contact force acting on each sphere, $\boldsymbol{r}_{cp,n}$: position vector from the gravity center of stone to the contact point.

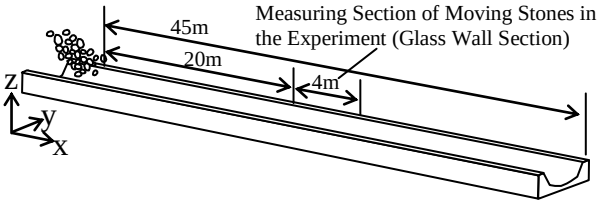

Figure 7 Shape of the experimental channel

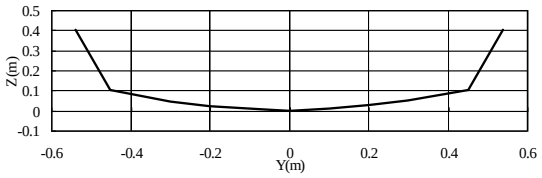

Figure 8 Channel cross section

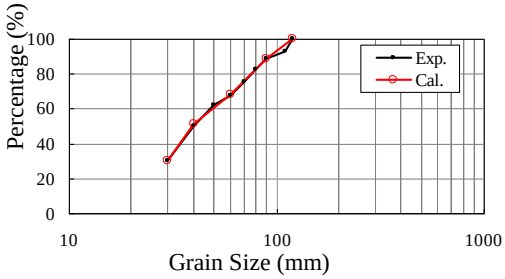

Figure 9 Grain size distributions

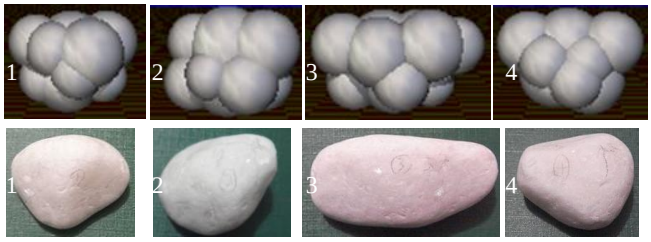

Figure 10 Shapes of stones

Table 1 Parameters used in the simulation

$\Delta x, \Delta y, \Delta z$:Fluid Calculation cell Size for One Stone Moving Simulation	0.02	m	$\Delta x, \Delta y, \Delta z$:Fluid Calculation cell Size for a Cloud of Stone Simulation	0.01	m
Δt :Time Step for Fluid Calclation	1.0×10^{-4}	s	C_s :Smagorinsky Coefficient	0.173	—
ρ_w :Density of Water	1,000	kg/m^3	$\Delta t'$:Time Step for DEM Calclation	1.0×10^{-6}	s
ρ_s :Density of Stone	2,650	kg/m^3	E :Elastic Modulus	5.0×10^{10}	Pa
μ_w :Viscosity Coefficient of Water	8.9×10^{-4}	kg/m^3	pos:Poisson's Ratio	0.33	—
μ_s :Viscosity Coefficient of Stone	8.9×10^{-4}	Pa·s	h:Coefficient of Dashpot	0.11	—

Contact forces between stones are calculated by the Discrete Elements Method (Cundall and Strack, 1979) and the spring constants and coefficients of dashpot are calculated by equations (13)-(15) (Gotoh, 2004):

$$k_n = \left\{ \frac{4}{9} \left(\frac{r_1 r_2}{r_1 + r_2} \right) \left(\frac{E}{1 - pos^2} \right)^2 e_n \right\}^{\frac{1}{3}} \tag{13}$$

$$s_0 = \frac{k_s}{k_n} = \frac{1}{2(1 + pos)} \tag{14}$$

$$c_n = 2h \sqrt{\frac{m_1 m_2}{m_1 + m_2} k_n} \quad , \qquad c_s = c_n \sqrt{s_0} \tag{15}$$

where suffix n :a component of direction from center of spheres to the contact point, suffix s :orthogonal two directions on the tangential plane, r_1 , r_2 :radii of contacting two spheres m_1 , m_2 :mass of contacting spheres.

3. APPLICATION TO REAL SCALE EXPERIMENT

3.1 The Condition of the Numerical Analysis

Figure 7 shows the experimental channel with 45m long and 1:20 bed gradient (Fukuoka et al., 2005). In the experiments, moving trajectories of stones were measured in the glass wall section. Figure 8 shows the channel cross section. In the numerical analysis, the coordinate system is defined as x axis in the longitudinal direction and z axis in the vertical direction of the channel bed, as shown in Figure 7. We simulated by the model for 38m long from upstream end to the downstream end of the channel. In order to reproduce coarse aggregates of the experimental channel bed exposed by rolling stones, simulation channel bed is composed of spheres with irregular radii and height varying in the range of 0.02m. The discharge of $0.5m^3/s$ is given at the upstream end of the channel, and zero pressure intensity is given at the downstream end. Figure 9 shows the grain size distribution of supplied stones into the simulation channel. The diameters of the irregularly shaped stones are given as corresponding sphere diameters with the same volume. In the simulation, 4 different types of stone-shapes which are composed of 8-9 small spheres are prepared as shown in Figure 10. Stones supplied at the upstream end of the simulation channel are 360kg in 4 seconds as well as the experiment. In the real scale experiment, the motion of one stone in streams was also investigated.

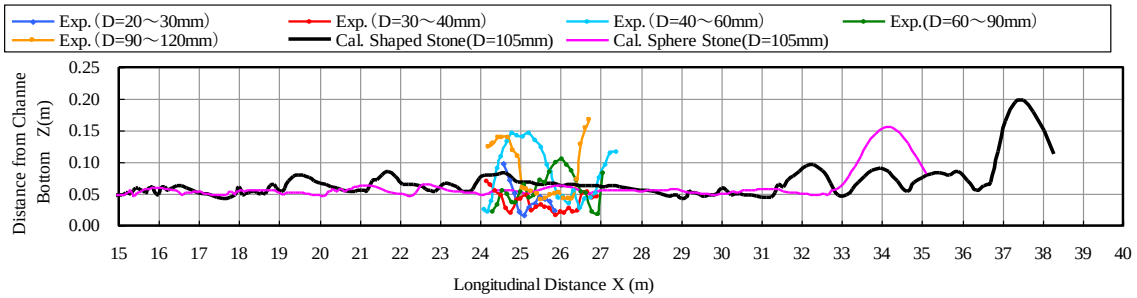

Figure 11 The Trajectories of one stone (x-z plane)

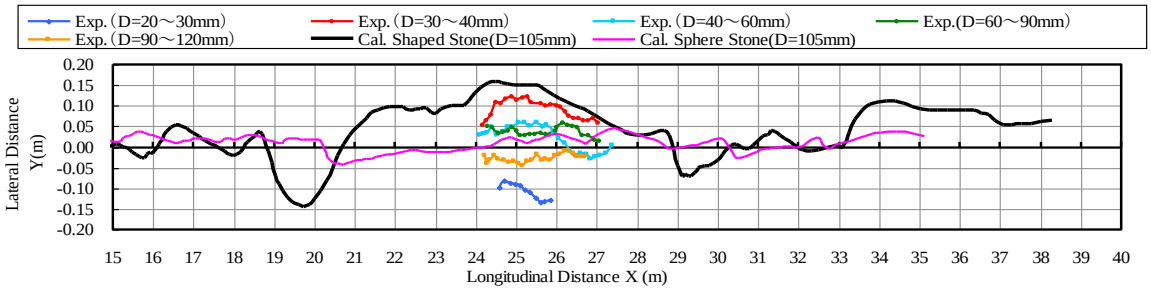

Figure 12 Trajectories of one stone (x-y plane)

Effects of the stone shape on one stone motion are established by the comparison of simulation results of No.1 stone in Figure 10 and a spherical stone. Table 1 shows the parameters used in the simulation. The time step of discrete element method is set one hundredth of time step of flow calculation which keeps simulated motion of stones stably.

3.2 One Stone Moving

Figure 11 and Figure 12 show the simulated trajectories of one stone moving in a stream with a shaped stone and a sphere on x-z plane and x-y plane, respectively. These figures also show measured trajectories of a stone measured by the experiment. The simulated shaped stone saltates frequently, and flow down a wide range across the channel as well as the experimental result. On the other hand, simulated spheres do not saltate so frequently, and flow down just only the center of the channel, which reveals the importance of shape of stones on the stone motion. The reason of the difference of trajectories between the shaped and sphere stones arises from that the frontal area of the shaped stone is larger than that of the sphere stone with the same volume, and the shaped stone can saltate due to the collision with the channel bottom in irregular manner for the different shape from spheres. It is concluded that stones shapes are significant effects on their motions in streams.

3.3 A cloud of Stones Moving

The numerical model is applied to the movement of a cloud of stones in the real scale experiment (Fukuoka et al., 2005). Figure 13 is the snap shot of the simulated stones moving in the stream. In the experiment, all of supplied stones reached downstream end of the channel in about 20 seconds. However in the simulated results, some small stones remained at the supplying section in 20 seconds after stones supply. This is because fluid cells size of calculation is a little bit larger than the suitable size for calculating fluid motion around small spheres. Therefore, we investigate interactions between moving stones and streams at sufficient downstream sections. Figure 14 shows the comparison of experimental and numerical vertical distribution of stone velocity. The figure also shows a simulated water velocity distribution. The simulated stones velocities indicate almost the same value as the experimental values which become almost uniform in vertical direction. Figure 15 shows vertical distributions of existence probabilities of stones. The simulated existence probabilities of stones for D < 60mm (D=30mm-60mm) are larger around the bottom and smaller at the upper position than those of the experiment. However, for D>60mm (D=60mm-90mm, 90mm-120mm), the simulated probabilities have good agreement with those of the experiment.

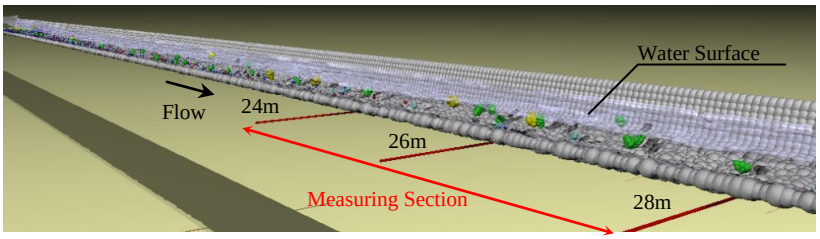

Yellow :D=90-120m
Green :D=60-90m
Light Blue :D=40-60m
Red :D=30-40m
Blue :D=20-30m

The channel wall is not shown in the figure.

Figure 13 Snap shot of the measuring stones section in the analysis

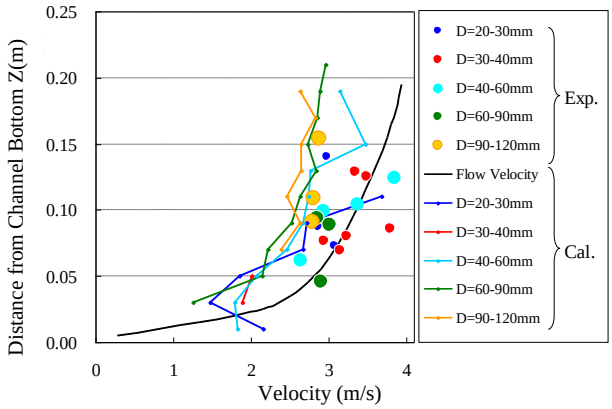

Figure 14 Vertical distributions of stones velocity

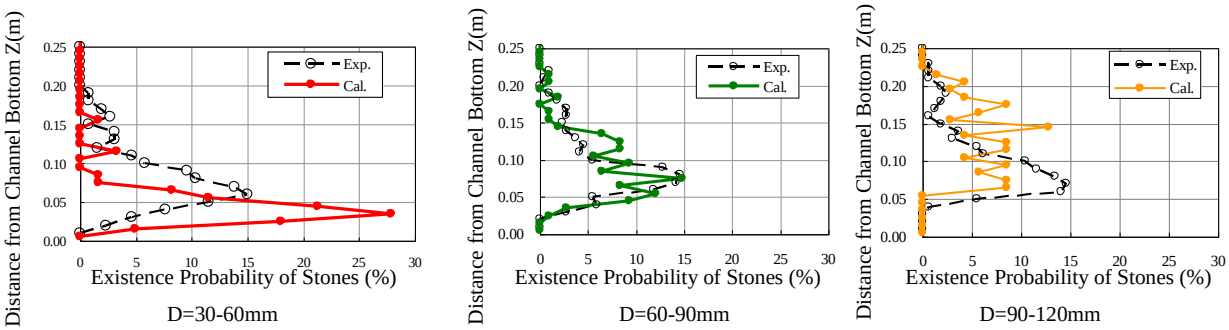

Figure 15 Vertical distributions of existence probabilities of stones

3.4 Discussions of Moving Mechanism of Stones in Stream

The stones moving mechanism is discussed by the simulation and the experiment. At first, forces acting on the stones and stones moving configuration are investigated. Figures 16 and 17 show simulated vertical distribution of volume density of stones, forces acting on stones in unit volume in x and z directions, respectively. In Figure 17, total forces in x and z directions change to the opposite direction around middle of the depth. The direction of the forces acting on stones is upstream-upward direction in the lower part of the depth and downstream direction in the upper part of the depth. Figure 18 shows stones trajectories relative to the viewer moving with the average stone velocity 2.65m/s. Stones move to the upstream-upward direction and fall to the downstream direction to the average stone velocity.

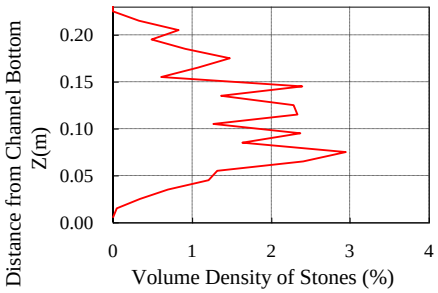

Figure 16 Vertical distribution of volume density of stones

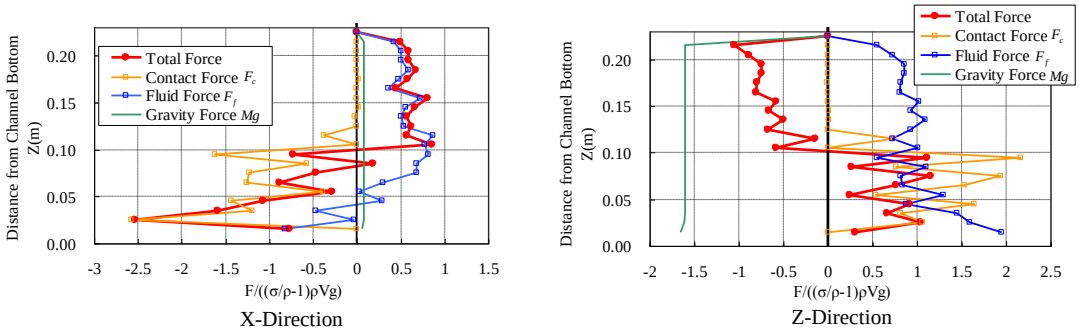

Figure 17 Vertical distributions of forces acting on stones

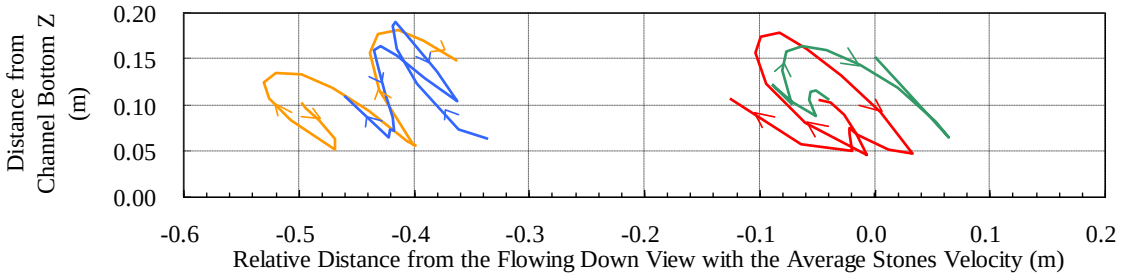

Figure 18 Stones Trajectories relative to the viewer moving with stone velocity

Next, the mechanism of stones-water multiphase flow is discussed. Figure 19 shows x and z directional forces acting on a unit volume evaluated at the center of the channel on time average. Contact forces F_c calculated by eq. (12) are evaluated at gravity center of stones. Contact force in the x-direction is larger near the bottom. On the other hand, momentum exchange by the stones is larger around the middle part of the depth. Apparent shear stress and normal stress distributions are shown in Figure 20. Here, the apparent stresses are calculated by the integration of the forces shown in Figure 19 from the water surface to the bottom with the assumption of little variation of time-averaged multiphase flow structures in x and y directions. In other words, the shear stress and normal stress are described by net momentum exchanges in x and z directions across the z isosurface, respectively. From these figures, the ratio of contact forces to the total shear stress is larger than the ratio of contact forces in normal stress. The above indicates that the hydrodynamic force acting on stones in x-direction is much larger than that in z-direction, and the stream-wise momentum of stones are transported by collisions. It is noticed that despite just only 1-2% of the stones volume density, the ratio of contact force and momentum exchange between stones to the total shear stress becomes almost 70% around the bed. In other words, stones with a few percent of volume density in streams play a significant effect on vertical momentums transport.

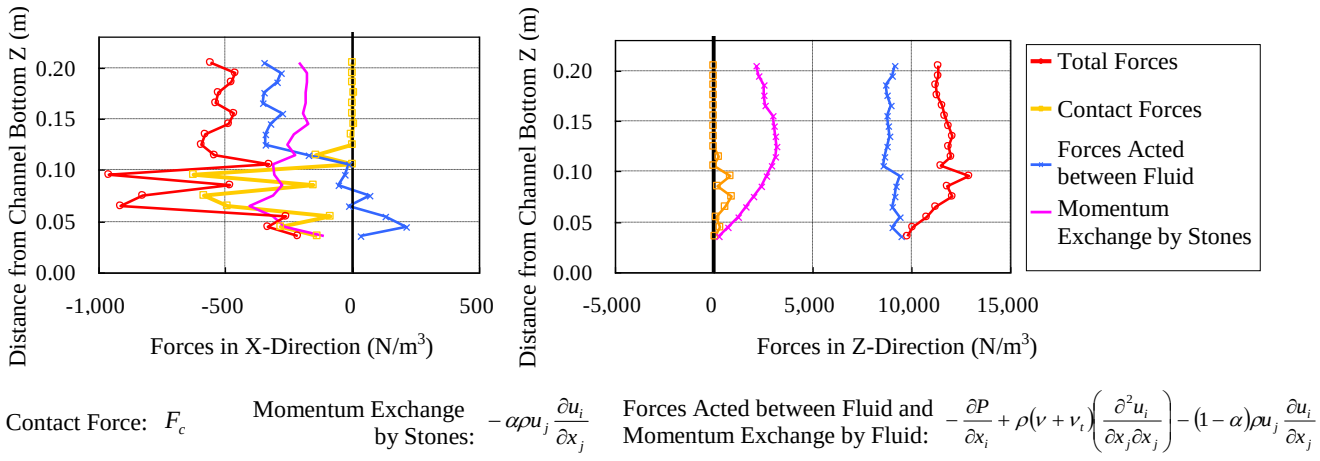

Figure 19 Vertical distributions of forces in stones-stream multiphase flow

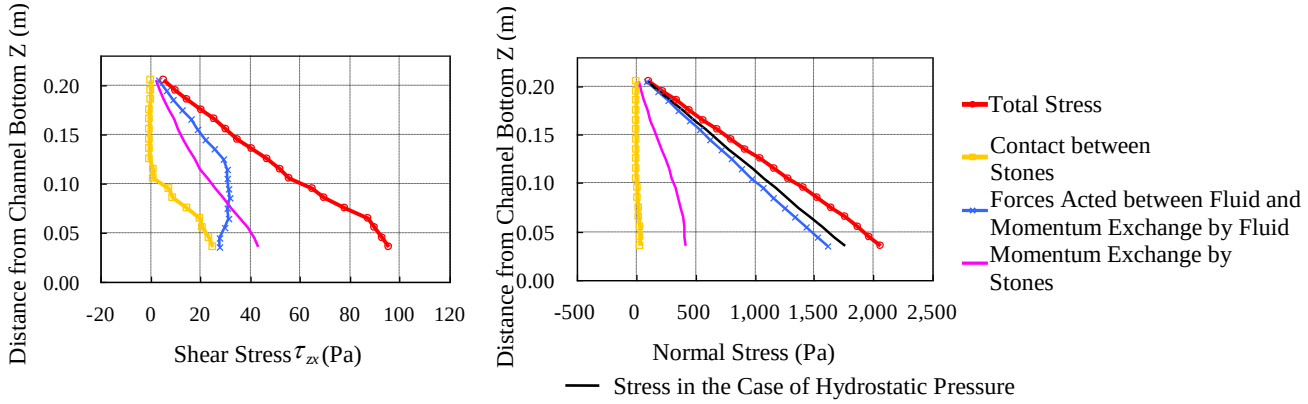

Figure 20 Vertical distributions of stress

4. CONCLUSION

The three-dimensional numerical model for flows with shaped stones was developed and applied to the result of real scale experiment regarding stones moving in streams. The model gave good explanations to the results of real scale experiment, such as stones trajectories, vertical distributions of velocities and existences probabilities of stones. From the investigation of one stone moving in streams, it was clarified that experimental trajectory with frequent saltation and lateral migration could not be reproduced in the simulation unless the irregular stone shape is considered. It was demonstrated that the motion of stones with just a few percent of volume density in streams plays a significant role of vertical momentums transport from the consideration of dynamic mechanism of a cloud of stone moving in streams.

REFERENCES

Cundall,P.A. and Strack,O.D.L. (1979) A discrete numerical model for granular assemblies, Geotechnique, Vol.29, No.1, pp.47-65.

Gotoh,H., Yeganeh,A. and Sakai,T. (2000) Coupling of Multiphase-Flow Model and Distinct Element Method for Simulation of Sediment Transport under High Bottom Shear, Proceedings of JSCE, Vol. 649/II-51, pp.17-26, in Japanese.

Gotoh,H. (2004) Computational Mechanics of Sediment Transport, Morikita Shuppan Co.,Ltd., in Japanese.

Fukuoka,S., Watanabe,A., Shinohara,Y., Yamashita,S. and Saitou,K. (2005) Movement Mechanism for a Mass of Gravel Flow with High Speed and Estimation of Chanel Bed Abrasion, Proceedings, Advances in River Engineering, JSCE, Vol.16, pp.291-296, in Japanese.

Hirt,C.W. and Nichols,B.D. (1981) Volume of Fluid(VOF)Method for the Dynamics of Free Boundaries, J.Comput.Phys., 39, pp.201-225.

Kajishima,T., Takiguchi,S., Hamasaki,H. and Miyake,Y. (2001) Turbulence Structure of Particle-Laden Flow in a Vertical Plane Channel Due to Vortex Shedding, JSME Series B, Vol.44, No.4 pp.526-535.

Suzuki,K., Kubota,J. and Ohtsubo,H. (2003) Voxel based collision detection algorithm for rigid body simulation, J. Applied Mechanics, JSCE, Vol.6, pp.131-139, in Japanese.

Matsushima,T., Katagiri,J., Uesugi,K., Tsuchiyama,A. and Nakano,T. (2009) 3D Shape Characterization and Image-Based DEM Simulation of the Lunar Soil Simulant FJS-1 J.Aerospace Engineering, Vol. 22, No. 1, pp. 15-23.

Ushijima,S., Fukutani,A. and Makino,O. (2008) Prediction Method for Movements with Collisions of Arbitrary-Shaped Objects in 3D Free-Surface Flows Proceedings, JSCE, B Vol.64 No.2 pp.128-138, in Japanese.